

# High-Order Implicit Time-Marching Methods Based on Generalized Summation-By-Parts Operators

Pieter D. Boom<sup>a,\*</sup>, David W. Zingg<sup>a,\*\*</sup>

<sup>a</sup>*Institute for Aerospace Studies, University of Toronto, Toronto, Ontario, M3H 5T6, Canada*

---

## Abstract

This article extends the theory of generalized summation-by-parts (GSBP) operators and simultaneous approximation terms for application to initial-value problems. The generalized framework includes both classical finite-difference (FD) SBP operators as well as those that: 1) have no repeating internal stencil; 2) have nonuniform nodal distributions in the computational domain; and 3) have nodal distributions which do not include one or both boundary points. This unified class of SBP operators enables the construction of high-order, unconditionally-stable, implicit time-marching methods which require significantly fewer fully-coupled solution points than time-marching methods based on classical FD-SBP operators and hence can be more efficient. In this article it is shown that the stability and accuracy properties of time-marching methods based on classical FD-SBP operators extend to those based on GSBP operators. This specifically includes linear stability of all dual-consistent discretizations and nonlinear stability of dual-consistent discretizations with a diagonal norm. Furthermore, the superconvergence of linear functionals of the solution integrated with the quadrature associated with the norm is extended for the GSBP framework, and the superconvergence of multistage time-marching methods based on the multi-element approach is proven. Several model problems are simulated numerically to demonstrate the theoretical results of the article.

*Keywords:* Summation-by-Parts, Simultaneous-Approximation-Terms, Quadrature, Superconvergence, Implicit Time-Marching Methods,

---

\*Ph.D. Candidate

\*\*Professor and Director, Tier 1 Canada Research Chair in Computational Aerodynamics, J. Armand Bombardier Foundation Chair in Aerospace Flight

## 1. Introduction

Many dynamical systems in science and engineering are modelled by stiff initial value problems (IVPs) either directly or through semi-discretization of partial differential equations. The numerical solution of stiff IVPs is limited by the stability of the time-marching method employed, motivating the use of unconditionally-stable implicit methods. The computational cost and complexity of such methods is offset by the freedom to choose much larger time steps and therefore fewer time steps, limited only by the desired accuracy of the solution. This also motivates the use of higher-order methods, as larger time steps can be used to obtain the same level of accuracy. Recently, it was shown that high-order finite-difference (FD) operators satisfying the summation-by-parts (SBP) property can be applied as high-order unconditionally-stable implicit time-marching methods for application to stiff IVPs [41, 47].

Classical FD-SBP operators were first introduced in 1974 [38] and extended for different types of norms in 1994 [51] as a means to derive stable and efficient boundary closures for high-order FD schemes. For practical problems, these operators are often augmented with simultaneous approximation terms (SATs) to weakly enforce boundary conditions and multiblock interface coupling [11, 12, 21, 22]. The appeal of the FD-SBP-SAT approach for large-scale complex numerical simulations is the ability, under certain restrictions, to prove time stability in curvilinear coordinate systems [52], obtain superconvergence of linear functionals [5, 31, 33, 41], and to minimize interblock communication overhead, as only boundary information is required to enforce boundary conditions and interface coupling. As a result, this approach has been applied to a variety of numerical simulations, for example in computational fluid dynamics [30, 46, 48, 53, 54]. Furthermore, several notable contributions and extensions to the classical FD-SBP-SAT theory have been made, for example application to higher-order derivatives [17, 18, 35, 42, 44, 45]. Comprehensive review articles on the SBP-SAT approach are available in [16] and [55].

The motivation for applying the FD-SBP-SAT approach in time is the ability to construct high-order, provably stable time-marching methods for which fully-discrete energy estimates of PDEs can be obtained when the approach is used for the spatial discretization as well [47]. It was shown in [41] that all dual-consistent time-marching methods based on classical FD-SBP operators are unconditionally stable for linear problems, provide damping of stiff modes, and those with a diagonal norm satisfy certain nonlinear stability criteria as well. In general, the approach leads to a global discretization of the problem in time [47]: the solution at any point in time is fully coupled to all other solution points. This can be prohibitively expensive, but if a dual-consistent multi-block formulation is used, a more efficient local approach is obtained and the solution remains coupled only within each block [41]. What remains to be seen is the relative efficiency of this approach with respect to traditional time-marching methods given that the minimum block sizes of the classical FD-SBP-SAT approach are quite large.

In [15] a generalized framework was presented which extends the theory of classical FD-SBP operators to include operators which 1) have no repeating internal stencil; 2) have nonuniform nodal distributions in the computational domain; and 3) have nodal distributions which do not include one or both boundary points. Individually these ideas are not unique; for example collocated-pseudo-spectral methods, which have neither a repeating internal stencil nor a uniform nodal distribution, satisfy the SBP condition and have been used in conjunction with SATs [9, 10, 27, 28, 29]. Furthermore, Reichert *et al.* [50] developed an approach for FD-SBP-SAT discretizations on over-set grids where the operators may not include one or both boundary points. This was based on the earlier work of Abarbanel *et al.* [1, 2] and is similar to work presented in [3, 4, 19]. Del Rey Fernández *et al.* [15], however, go on to explore the deep link between the norm of the generalized SBP (GSBP) operators and an associated quadrature, initially observed in [31] for classical FD-SBP operators and used implicitly with approaches like collocated-pseudo-spectral methods. Furthermore, they prove the existence of GSBP operators given a nodal quadrature and show that the maximum order of the resulting operator is defined by the order of the associated quadrature.

Time-marching methods based on GSBP operators have some desirable properties for stiff IVPs in addition to those of time-marching methods based on classical FD-SBP operators. Most important is that high-order GSBP op-

| Operator               | Norm  | Ext.    | Order Quad.          | Order <sub>Max.</sub> Operator | Range of $n$   |
|------------------------|-------|---------|----------------------|--------------------------------|----------------|
| FD-SBP [38]            | Diag. | –       | $n/2$                | $n/4$                          | 8, 12, 16      |
| FD-SBP [51]            | Block | –       | $n/2$                | $n/2 - 1$                      | 8, 12, 16, ... |
| Optimized FD-SBP [43]  | Diag. | 2       | $(n - 2)/2$          | $(n - 2)/4$                    | 6, 10, 14      |
| Newton-Cotes GSBP [15] | Diag. | 1       | $2\lceil n/2 \rceil$ | $\lceil n/2 \rceil$            | 2, ..., 8, 10  |
| Newton-Cotes GSBP [15] | Dense | 1       | $2\lceil n/2 \rceil$ | $n - 1$                        | $\geq 2$       |
| Lobatto GSBP [10, 23]  | All   | 1, 2    | $2n - 2$             | $n - 1$                        | $\geq 2$       |
| Gauss GSBP [15]        | Diag. | 1, 2, 3 | $2n$                 | $n - 1$                        | $\geq 2$       |

Table 1: Comparison of classical FD-SBP operators and GSBP operators, where  $n$  is the minimum required number of nodes in the operator, and the extensions (Ext.) referred to in the table are: 1) no repeating internal stencil; 2) nonuniform nodal distributions in the computational domain; and 3) nodal distributions which do not include one or both boundary points.

erators require significantly fewer nodes than equivalent classical FD-SBP operators, minimizing the number of fully coupled solution points and maximizing efficiency. Consider the examples in Table 1. This limited set of operators demonstrates that GSBP operators can be constructed that are two times smaller than classical FD-SBP operators of the same order, and this ratio is nearly four when only diagonal-norm operators are considered. For example, GSBP operators based on Lobatto quadrature rules require two times fewer nodes than classical block-norm FD-SBP operators to achieve the same order and nearly four times fewer than classical diagonal-norm FD-SBP operators. Furthermore, in the present article it is shown that the convergence rate of linear functionals is limited by the minimum of: 1) the required order of quadrature rules associated with GSBP operators, and 2) one plus twice the order of the GSBP operators themselves. Therefore, the reduction in the number of nodes required to obtain a given order of convergence is amplified for linear functionals. For example, GSBP operators based on Gauss quadrature rules require approximately four times fewer nodes than both diagonal and block-norm classical FD-SBP operators to achieve the same convergence rate for linear functionals.

The objective of this paper is to show that high-order implicit time-marching methods based on GSBP operators can be more efficient than those based on classical FD-SBP operators while retaining the stability properties of the latter. This is accomplished by extending the theory of the GSBP framework presented in [15] to application to IVPs. Specifically, the goal is to show that the generalized approach maintains linear stability of all dual-consistent discretizations and nonlinear stability of those based on diagonal norms, stability of the multi-block approach, and superconvergence of linear functionals proven for the classical FD-SBP-SAT approach in [41, 47].

The paper is organized as follows: Section 2 gives a brief review of the GSBP approach presented in [15] in the context of IVPs. The accuracy and stability of time-marching methods based on classical FD-SBP operators is extended to those based on GSBP operators in Sections 3 through 5. Numerical examples are presented in Section 6 to demonstrate various elements of the theory developed in the article. A summary concludes the paper in Section 7.

## 2. The GSBP-SAT Approach

This article considers discrete approximations of IVPs for nonlinear non-autonomous systems of ordinary differential equations:

$$\mathcal{Y}' = \mathcal{F}(\mathcal{Y}, t), \quad \mathcal{Y}(T_1) = f_{T_1}, \quad \text{with } T_1 \leq t \leq T_2, \quad (1)$$

where  $\mathcal{Y} \in \mathbb{C}^M$ ,  $\mathcal{Y}' = \frac{d\mathcal{Y}}{dt}$ ,  $\mathcal{F}(\mathcal{Y}, t) : \{\mathbb{C}^M, \mathbb{R}\} \rightarrow \mathbb{C}^M$ , and  $f_{T_1}$  is the vector of initial data.

Note that in this article we make the distinction between diagonal and nondiagonal-norm matrices. The latter will be referred to as dense norms following [15], but encompasses all nondiagonal norms whether they are strictly dense matrices or not. For example, classical FD-SBP operators with a full, or restricted-full norm are referred to as dense-norm operators.

### 2.1. Generalized Summation-By-Parts Operators

The motivation behind summation-by-parts (SBP) operators is to be able to apply the energy method to determine the stability of the numerical solution to ordinary and partial differential equations. In the continuous

case, provided that a unique solution exists, stability implies well-posedness [24, 25, 37]. SBP is a discrete analogue of integration-by-parts, which enables us to relate the numerical quadrature to boundary data. In [15] a generalized definition of SBP (GSBP) was introduced:

$$\mathbf{u}^* H D \mathbf{v} + \mathbf{u}^* D^T H \mathbf{v} = \mathbf{u}^* \tilde{E} \mathbf{v} \approx \bar{U} \mathcal{V} \Big|_{T_1}^{T_2}, \quad (2)$$

where  $\mathbf{u}^*$  is the conjugate transpose of  $\mathbf{u}$ , and  $D$  is a linear first-derivative GSBP operator defined as:

**Definition 1. Generalized summation-by-parts operator [15]:** *An operator  $D$  is an order  $q$  GSBP approximation to the first derivative on the nodal distribution  $\mathbf{t} = [t_1, \dots, t_n]$ , provided that all  $t_i$  are unique, if  $D$  satisfies:*

$$D \mathbf{t}^j = j \mathbf{t}^{j-1}, \quad j \in [0, q], \quad (3)$$

with  $q \geq 1$ ,  $H$  is an SPD matrix which defines a discrete inner product and norm:

$$(\mathbf{u}, \mathbf{v})_H = \mathbf{u}^* H \mathbf{v}, \quad \|\mathbf{u}\|_H^2 = \mathbf{u}^* H \mathbf{u}, \quad (4)$$

and  $(HD + D^T H) = \tilde{E}$  such that

$$(\mathbf{t}^i)^* \tilde{E} \mathbf{t}^j = (i + j) \int_{T_1}^{T_2} \tilde{t}^{i+j-1} d\tilde{t} = T_2^{i+j} - T_1^{i+j}, \quad i, j, \in [0, r], \quad (5)$$

with  $r \geq q$ .

This differs from the classical SBP definition in that  $\tilde{E}$  is not required to be exact for all  $i, j \geq 0$ , and therefore  $\mathbf{u}^* \tilde{E} \mathbf{v}$  may only be an approximation of  $\bar{U} \mathcal{V} \Big|_{T_1}^{T_2}$ . This definition encompasses classical FD-SBP operators, as well as others such as collocated-pseudo-spectral methods, and under certain restrictions, Discontinuous-Galerkin schemes (*e.g.* [23]). In this article the product  $HD$  will be denoted  $\Theta$ .

The existence of such operators was presented in [15]. The main results are: 1) all GSBP operators are associated with a nodal quadrature rule, and the minimum order  $\tau_{\min}$  of the associated quadrature rule is defined by the order  $q$  of the GSBP operator; and 2) given a nodal quadrature rule, a GSBP operator exists and the order of the operator  $q$  is defined by the order of the quadrature rule  $\tau$ . Sharper bounds on these results for dense-norm operators are used implicitly in this article and will be presented in a future manuscript.

The generalized framework relaxes the conditions on the nodal distribution and the requirements in the derivation of SBP operators, enabling the construction of both more efficient GSBP operators and associated nodal quadrature rules, first demonstrated in [15]. Note that efficiency of an operator in this article is taken as the order of accuracy versus the minimum number of nodes required in the operator.

## 2.2. Generalized Simultaneous Approximation Terms

Applying a GSBP approach to the temporal derivative of the IVP (1) necessitates a means to impose the initial data. A common approach is to use simultaneous-approximation-terms (SATs) [41, 47] which weakly impose the initial data via penalty terms.

To apply the SAT technique requires an approximation of the individual boundary values  $\tilde{y}_{T_1} \approx \mathcal{Y}(T_1)$  and  $\tilde{y}_{T_2} \approx \mathcal{Y}(T_2)$ . In the classical approach this is obtained from the solution values  $y_{d,0}$  and  $y_{d,n}$ ; however, in the case where the nodal distribution does not include one or both boundary points, these values must be extrapolated [3, 4, 15, 19, 50]. Here, an extrapolation operator is defined by

$$s_{T_1}^T \mathbf{t}^j = T_1^j \quad \text{and} \quad s_{T_2}^T \mathbf{t}^j = T_2^j, \quad j \in [0, n-1]. \quad (6)$$

Following [15], the fully-discrete form of (1) can then be written as

$$(D \otimes I_M) \mathbf{y}_d = \mathbf{F}_d - \sigma(H^{-1} s_{T_1} \otimes I_M)((s_{T_1}^T \otimes I_M) \mathbf{y}_d - (I_n \otimes f_{T_1})), \quad (7)$$

with

$$\mathbf{y}_d = \begin{bmatrix} y_{d,1} \\ \vdots \\ y_{d,n} \end{bmatrix}, \quad \mathbf{F}_d = \begin{bmatrix} \mathcal{F}(y_{d,1}, t_1) \\ \vdots \\ \mathcal{F}(y_{d,n}, t_n) \end{bmatrix}, \quad y_{d,i} = \begin{bmatrix} y_{d,k,1} \\ \vdots \\ y_{d,k,M} \end{bmatrix}, \quad (8)$$

where  $n$  is the number of nodes in the operator  $D$ ,  $\sigma$  is the SAT penalty parameter, and  $s_{T_1}$  is the extrapolation operator defined above. A convenient vector decomposition of  $\tilde{E} = \Theta + \Theta^T$  is:

$$\tilde{E} = \Theta + \Theta^T = s_{T_2} s_{T_2}^T - s_{T_1} s_{T_1}^T, \quad (9)$$

which relates the definition of the derivative operator and form of the SAT terms through the extrapolation operators. To the authors' knowledge, this specific decomposition was first proposed in [15], though others have used extrapolation operators for FD and FD-SBP schemes [3, 4, 19, 50] and have used  $\tilde{E}$  which are not equal to  $\text{Diag}[-1, 0, \dots, 0, 1]$  [1, 2]. This formulation of both  $\Theta$ , *i.e.* that it have the property  $\Theta + \Theta^T = s_{T_2} s_{T_2}^T - s_{T_1} s_{T_1}^T$ , and of the SAT terms is assumed for the rest of this article. The conservation, time-stability, and consistency of this approach is discussed in [15], and the choice of SAT parameter for stability of time-marching methods based on GSBP operators of this form is addressed further in Section 4.

### 3. Accuracy

The additional freedom granted by the generalized framework in choosing a nodal distribution and relaxing the requirements in the derivation of SBP operators enables the construction of more efficient operators and associated quadrature rules. This section builds on this premise and extends various formal accuracy results of time-marching methods based on classical FD-SBP operators to those based on GSBP operators. The primary goal is to extend the superconvergence theory of linear functionals, first shown for FD-SBP-SAT discretizations of initial boundary value problems in [32] and extended for IVPs in [41]. The motivation for this theory stems from the fact that in many numerical simulations, integrated quantities are often of more interest than the solution itself. In addition, the superconvergence of linear functionals implies that the solution at block boundaries is superconvergent, analogous to a Runge-Kutta method with lower stage-order and a higher-order solution update. This is another motivation for using a multi-block



or multi-element approach with small block sizes, as more solution points become high order. These results amplify the efficiency of the GSBP operators. The proof of superconvergence requires several intermediate results which are presented in the subsections below. Finally, the section ends with a brief discussion of the accuracy of problems with stiff source terms.

### 3.1. Pointwise Accuracy

This section introduces some useful definitions related to the error of the numerical solution, which will be used in future sections, and formalizes the pointwise accuracy of the solution. To begin, consider a scalar IVP which is linear with respect to the solution:

$$\mathcal{Y}' = \lambda \mathcal{Y} + \mathcal{G}(t), \quad \mathcal{Y}(T_1) = f_{T_1}, \quad \text{with } T_1 \leq t \leq T_2, \quad (10)$$

where  $\mathcal{Y}(t) \in \mathbb{C}$  and  $\mathcal{G}(t) : \mathbb{R} \rightarrow \mathbb{C}$ , for which the GSBP-SAT discretization is:

$$D\mathbf{y}_d = \lambda \mathbf{y}_d + \mathcal{G}(\mathbf{t}) + \sigma H^{-1} s_{T_1} (s_{T_1}^T \mathbf{y}_d - f_{T_1}). \quad (11)$$

This will be referred to as the primal problem. The truncation error is defined by replacing the discrete solution in (11) with the continuous solution projected onto the nodal distribution,  $\mathbf{y}$ , and rearranging to obtain:

$$\begin{aligned} T_e &= D\mathbf{y} - \lambda \mathbf{y} - \mathcal{G}(\mathbf{t}) - \sigma H^{-1} s_{T_1} (s_{T_1}^T \mathbf{y} - f_{T_1}) \\ &= D\mathbf{y} - \sigma H^{-1} s_{T_1} (s_{T_1}^T \mathbf{y} - f_{T_1}) - \mathbf{y}', \end{aligned} \quad (12)$$

which is by definition of minimum uniform order  $q$ . This differs slightly from the classical SBP-SAT definition in [41],  $T_e = D\mathbf{y} - \mathbf{y}'$ , since  $s_{T_1}^T \mathbf{y}$  is not necessarily equal to  $f_{T_1}$ . The goal now is to determine the pointwise accuracy of the numerical solution. This is accomplished by examining the error between the numerical solution and exact solution, which can be defined in terms of (12) as:

$$e = \mathbf{y} - \mathbf{y}_d = (\Theta - \sigma s_{T_1} s_{T_1}^T - \lambda H)^{-1} H T_e. \quad (13)$$

Using extensions of Assumption 2 and Corollary 1 from [41] the pointwise accuracy of the discrete solution can be summarized with following theorem:

**Theorem 1.** *The pointwise accuracy of a GSBP-SAT discretization (11) of the IVP (10) using a GSBP operator of order  $q$  and a compatible SAT implementation is of order  $q$  provided an extension of Assumption 2 from [41] holds for GSBP operators.*

*Proof.* The proof is analogous to Proposition 5 in [41] without making a distinction between interior and boundary components of the operator.  $\square$

This is not a surprising result as GSBP operators and SAT terms are constructed to be of order  $q$ . Nevertheless it is an important result for two reasons: 1) it is important to note that this result is not as strong as Proposition 5 in [41] since there is not such a clear distinction in general between interior and boundary components of GSBP operators as there is with classical FD-SBP operators; and 2) this result highlights the importance of Theorem 12 presented in Section 5, which shows that the pointwise accuracy of multi-element discretizations is one order higher,  $q + 1$ .

### 3.2. The Dual Problem

This section presents a brief review of the dual problem, a key tool required for proving the superconvergence of linear functionals in Section 3.3. The derivation of the continuous dual problem

$$-\Phi' = \bar{\lambda}\Phi + \mathcal{H}(t), \quad \Phi(T_2) = \bar{\alpha}, \quad \text{with } T_1 \leq t \leq T_2. \quad (14)$$

and dual functional

$$\mathcal{J}(\mathcal{Y}) = (\Phi, \mathcal{G}) + \bar{\Phi}\mathcal{Y}|_{T_1} = \mathcal{J}(\Phi). \quad (15)$$

can be found in several references (*e.g.* [31]). The challenge is to derive the discrete dual problem and functional for the generalized framework. A functional of the discrete primal problem (11) is defined as

$$J_H(\mathbf{y}_d) = (\mathcal{H}(\mathbf{t}), \mathbf{y}_d)_H + \alpha s_{T_2}^T \mathbf{y}_d. \quad (16)$$

Subtracting the discrete inner product of the discrete primal problem (11)

and a vector  $\phi_d$  leads to

$$\begin{aligned} J_H(\mathbf{y}_d) = & (\mathcal{H}(\mathbf{t}), \mathbf{y}_d)_H + \alpha s_{T_2}^T \mathbf{y}_d \\ & - (\phi_d, D\mathbf{y}_d - \lambda \mathbf{y}_d - \mathcal{G}(\mathbf{t}) - H^{-1} \sigma s_{T_1} (s_{T_1}^T \mathbf{y}_d - f_{T_1}))_H. \end{aligned} \quad (17)$$

Making use of GSBP, the relation  $\Theta + \Theta^T = \tilde{E} = s_{T_2} s_{T_2}^T - s_{T_1} s_{T_1}^T$ , and simplifying gives

$$\begin{aligned} J_H(\mathbf{y}_d) = & (\phi_d, \mathcal{G}(\mathbf{t}))_H - \sigma \phi_d^* s_{T_1} f_{T_1} \\ & + (H^{-1} (\Theta + (\sigma + 1) s_{T_1} s_{T_1}^T + \bar{\lambda}) \phi_d - H^{-1} s_{T_2} (s_{T_2}^T \phi_d - \bar{\alpha}) + \mathcal{H}(\mathbf{t}), \mathbf{y}_d)_H. \end{aligned} \quad (18)$$

This is deconstructed by extracting a discrete approximation to the dual functional:

$$J_H(\mathbf{y}_d) = (\phi_d, \mathcal{G}(\mathbf{t}))_H - \sigma \phi_d^* s_{T_1} f_{T_1} = J_H(\phi_d), \quad (19)$$

which leaves the discrete dual problem:

$$-D\phi_d = \bar{\lambda} \phi_d + \mathcal{H}(\mathbf{t}) - (1 + \sigma) H^{-1} s_{T_1} s_{T_1}^T \phi_d - H^{-1} s_{T_2} (s_{T_2}^T \phi_d - \bar{\alpha}), \quad (20)$$

which is a consistent analogue of the continuous dual problem and functional if  $\sigma = -1$ . This is called dual-consistency [40] and results in the dual problem:

$$-D\phi_d = \bar{\lambda} \phi_d + \mathcal{H}(\mathbf{t}) - H^{-1} s_{T_2} (s_{T_2}^T \phi_d - \bar{\alpha}), \quad (21)$$

and dual functional:

$$J_H(\mathbf{y}_d) = (\phi_d, \mathcal{G}(\mathbf{t}))_H + \phi_d^* s_{T_1} f_{T_1} = J_H(\phi_d). \quad (22)$$

With these definitions, the results of Section 3.1 can be extended for the discrete dual problem. The error in the dual-consistent discrete dual problem (21) can be defined as:

$$\tilde{e} = \phi - \phi_d = (-\Theta + s_{T_2} s_{T_2}^T - \bar{\lambda} H)^{-1} H \tilde{T}_e. \quad (23)$$

where the truncation error is:

$$\begin{aligned}\tilde{T}_e &= -D\phi - \bar{\lambda}\phi - \mathcal{H}(\mathbf{t}) + H^{-1}s_{T_2}(s_{T_2}^T\phi - \bar{\alpha}) \\ &= -D\phi + H^{-1}s_{T_2}(s_{T_2}^T\phi - \bar{\alpha}) + \phi',\end{aligned}\tag{24}$$

which is of minimum uniform order  $q$ . With this, the pointwise accuracy of the discrete dual problem (21) is summarized by the following theorem:

**Theorem 2.** *The pointwise accuracy of a dual-consistent GSBP-SAT discretization (21) of the continuous dual problem (14) using an GSBP operator of order  $q$  and a compatible SAT implementation, is of order  $q$ , provided an extension of Assumption 2 from [41] holds for GSBP operators.*

*Proof.* The proof follows from Theorem 1 analogously to Lemma 1 in [41].  $\square$

Again, this result is not surprising, as the operators are constructed to be of order  $q$ ; nevertheless, it is important for the same reasons as Theorem 1.

### 3.3. Superconvergence

This section extends the work of [31, 33, 41] on the superconvergence of linear functionals integrated with the quadrature associated with FD-SBP-SAT discretizations. Linear functionals are tightly linked with the dual problem as shown in Section 3.2 and also with the quadrature rule associated with GSBP operators. The accuracy with which GSBP norms can compute approximations of continuous L2 inner products, specifically inner products involving both the primal and dual problems, is critical. This motivates the following definition:

**Definition 2. Accuracy of a GSBP norm:** *The accuracy  $\rho$  of a norm  $H$  associated with a GSBP operator  $D = H^{-1}\Theta$  is the minimum order to which:*

- $(\mathbf{y}, \mathbf{z})_H$  approximates  $(\mathcal{Y}, \mathcal{Z})$ ; and
- $(\phi, D\mathbf{y} + H^{-1}s_{T_1}(s_{T_1}^T\mathbf{y} - f_{T_1}))_H$  approximates  $(\Phi, \mathcal{Y}')$ ,

where  $\Phi$  is the solution to the continuous dual problem (14), and  $f_{T_1}$  is the initial condition of the primal problem (10).

For diagonal norms associated with GSBP operators  $\rho = \min(2q + 1, \tau)$ , and for dense norms associated with GSBP operators  $\rho = \min(2q + 1, s)$ , where  $2\lceil q/2 \rceil \leq s \leq \tau$ . The derivation of these values, along with a more precise definition of  $s$  will be presented in a future article. Note however that  $\rho$  is always greater than or equal to the order of the GSBP operator itself.

To begin the investigation of the order to which linear functionals of GSBP-SAT discretizations converge, the dual problem is initially assumed to have homogeneous boundary conditions, *i.e.*  $\alpha = 0$ ; then the theory is extended for the non-homogeneous case. The convergence of linear functionals of the form  $\mathcal{J}(\mathcal{Y}) = (\mathcal{H}(t), \mathcal{Y})$  for  $\mathcal{H}(t) \in C^{\min(2q+1, \rho)}$  is addressed in the following extension of Proposition 7 from [41]:

**Theorem 3.** *If  $\mathbf{y}_d$  is the solution of a dual-consistent GSBP-SAT discretization (11) of the primal problem (10) with  $\text{Re}(\lambda) \leq 0$  and associated with a norm of order  $\rho$ , then the discrete functional  $J_H(\mathbf{y}_d) = (\mathcal{H}(\mathbf{t}), \mathbf{y}_d)_H$  is an order  $\min(2q+1, \rho)$  approximation of  $\mathcal{J}(\mathcal{Y}) = (\mathcal{H}(t), \mathcal{Y})$  for  $\mathcal{H}(t) \in C^{\min(2q+1, \rho)}$ .*

*Proof.* The proof follows analogously from Proposition 7 in [41]; however, there is a subtlety that is important to address: with the generalized operators,  $s_{T_1}^T \mathbf{y}$  does not always equal  $f_{T_1}$ . One of the key equations in the proof of Proposition 7 from [41] is,

$$(\phi_d, T_e)_H = (\tilde{T}_e, T_e)_H + (\phi, D\mathbf{y})_H - (\phi, \mathbf{y}')_H, \quad (25)$$

which in the generalized case becomes

$$(\phi_d, T_e)_H = (\tilde{T}_e, T_e)_H + (\phi, D\mathbf{y} + H^{-1}s_{T_1}(s_{T_1}^T \mathbf{y} - f_{T_1}))_H - (\phi, \mathbf{y}')_H. \quad (26)$$

The accuracy of this term is defined by Definition 2. In addition, the inner product of the truncation errors is no longer negligible and may become dominant if the order of the quadrature is significantly higher than the order

of the operator. Thus, using Definition 2 gives

$$\begin{aligned}
(\phi_d, T_e)_H &= \mathcal{O}(\Delta t^{\min(2q+1, \rho)}) + (\Phi, \mathcal{Y}') + \mathcal{O}(\Delta t^\rho) - ((\Phi, \mathcal{Y}') + \mathcal{O}(\Delta t^\rho)) \\
&= \mathcal{O}(\Delta t^{\min(2q+1, \rho)}) + \mathcal{O}(\Delta t^\rho) + \mathcal{O}(\Delta t^\rho) = \mathcal{O}(\Delta t^{\min(2q+1, \rho)}),
\end{aligned} \tag{27}$$

and the discrete functional  $J_H(\mathbf{y}_d) = (\mathcal{H}(\mathbf{t}), \mathbf{y}_d)_H$  becomes an order  $\min(2q+1, \rho)$  approximation of  $\mathcal{J}(\mathcal{Y}) = (\mathcal{H}(t), \mathcal{Y})$ .  $\square$

Given that the order of the diagonal norms associated with GSBP operators is at least twice that of the GSBP operator itself, this is a very useful result. To be explicit, the convergence of linear functionals of the form  $\mathcal{J}(\mathcal{Y}) = (\mathcal{H}(t), \mathcal{Y})$  for  $\mathcal{H}(t) \in C^{\min(2q+1, \rho)}$  computed from dual-consistent time-marching methods based on diagonal-norm GSBP operators is at least twice as high as the order of the time-marching method itself. On the other hand, dense norms associated with GSBP operators are not required to be significantly more accurate than the operator itself. This implies that in some cases dense-norm GSBP operators can be of higher order than diagonal-norm GSBP operators associated with the same quadrature rule; however, this also means that the rate of superconvergence is generally not as significant with respect to the order of the time-marching method.

Next, consider the accuracy of the numerical solution at the boundary of the domain  $s_{T_2}^T y_d = \tilde{y}_{T_2}$ , which in general is an extrapolation of the nodal solution values. This can be thought of as a solution update to an RK scheme which does not have a value of one in its abscissa. The goal is to extend Proposition 8 in [41], which shows that these values are superconvergent with the same rate as the linear functionals investigated above for dual-consistent time-marching methods based on classical FD-SBP operators. To simplify the proof of this extension, the following lemma is introduced, where  $\mathbf{1} = [1, \dots, 1]^T$ :

**Lemma 1.** *For a dual-consistent GSBP-SAT discretization,  $s_{T_2}^T (\Theta - \sigma s_{T_1} s_{T_1}^T)^{-1} = \mathbf{1}^T$ .*

*Proof.* Beginning with the assertion that  $s_{T_2}^T (\Theta - \sigma s_{T_1} s_{T_1}^T)^{-1} = \mathbf{1}^T$ , multiplying through by  $(\Theta + s_{T_1} s_{T_1}^T)$  and simplifying yields

$$s_{T_2}^T = \mathbf{1}^T (\Theta + s_{T_1} s_{T_1}^T). \quad (28)$$

Using the GSBP property, namely that  $\Theta + \Theta^T = \tilde{E}$ , yields

$$s_{T_2}^T = \mathbf{1}^T \left( -\Theta^T + \tilde{E} + s_{T_1} s_{T_1}^T \right), \quad (29)$$

and using the knowledge that GSBP operators are constructed such that  $\tilde{E} = s_{T_2} s_{T_2}^T - s_{T_1} s_{T_1}^T$  leads to

$$s_{T_2}^T = -(\Theta \mathbf{1})^T + \mathbf{1}^T s_{T_2} s_{T_2}^T. \quad (30)$$

A dual-consistent GSBP operator satisfies the identities  $D_1 \mathbf{1} = \Theta \mathbf{1} = \mathbf{0}$  and  $\mathbf{1}^T s_{T_2} = 1$ , eliminating the first term in the expression above and reducing the second term to  $s_{T_2}^T$ . An identity is obtained, proving the lemma.  $\square$

Using this result, the theorem which shows the superconvergence of the numerical solution at the domain boundary is now presented:

**Theorem 4.** *If  $\mathbf{y}_d$  is the solution of a dual-consistent GSBP-SAT discretization (11) of the primal problem (10) with  $\text{Re}(\lambda) \leq 0$  and associated with a norm of order  $\rho$ , then the solution extrapolated to the boundary  $\tilde{y}_{T_2} = s_{T_2}^T \mathbf{y}_d$  is an order  $\min(2q + 1, \rho)$  approximation of  $\mathcal{Y}(T_2)$ .*

*Proof.* Consider the discrete primal problem (11) with dual-consistent SAT value  $\sigma = -1$ . Rearranging, and left-multiplying by  $s_{T_2}^T$  gives

$$s_{T_2}^T y_d = \tilde{y}_{T_2} = s_{T_2}^T (\Theta + s_{T_1} s_{T_1}^T)^{-1} H (\lambda \mathbf{y}_d + \mathcal{G}(\mathbf{t}) + H^{-1} s_{T_1} f_{T_1}). \quad (31)$$

Using Lemma 1, yields

$$\tilde{y}_{T_2} = (\mathbf{1}, \lambda \mathbf{y}_d)_H + (\mathbf{1}, \mathcal{G}(\mathbf{t}))_H + \mathbf{1}^T s_{T_1} f_{T_1}. \quad (32)$$

Recall that  $\mathbf{1}^T s_{T_1} = 1$  for consistent GSBP operators. Furthermore, using

Theorem 3 and Definition 2 and simplifying yields

$$\begin{aligned}\tilde{y}_{T_2} &= (1, \lambda \mathcal{Y}) + (1, \mathcal{G}(t)) + f_{T_1} + \mathcal{O}(\Delta t^{\min(2q+1, \rho)}) \\ &= \int_{T_1}^{T_2} [\lambda \mathcal{Y} + \mathcal{G}(t)] dt + f_{T_1} + \mathcal{O}(\Delta t^{\min(2q+1, \rho)}).\end{aligned}\tag{33}$$

Substituting using the continuous primal problem (10) gives

$$\begin{aligned}\tilde{y}_{T_2} &= \int_{T_1}^{T_2} \mathcal{Y}' dt + f_{T_1} + \mathcal{O}(\Delta t^{\min(2q+1, \rho)}) \\ &= \mathcal{Y}(T_2) + \mathcal{O}(\Delta t^{\min(2q+1, \rho)}),\end{aligned}\tag{34}$$

thus completing the proof.  $\square$

Hence superconvergence is obtained not only for linear functionals, but also for the solution value at the boundary of the domain. This further motivates the use of a multiblock or multi-element discretization with small block sizes so that more solution points can be of significantly higher order. Finally, combining Theorems 3 and 4, the accuracy of the general linear functional  $J_H(\mathbf{y}_d) = (\mathcal{H}(\mathbf{t}), \mathbf{y}_d)_H + \alpha s_{T_2}^T \mathbf{y}_d$  follows immediately:

**Theorem 5.** *If  $\mathbf{y}_d$  is the solution of a dual-consistent GSBP-SAT discretization (11) of the primal problem (10) with  $\text{Re}(\lambda) \leq 0$  and associated with a norm of order  $\rho$ , then the discrete functional  $J_H(\mathbf{y}_d) = (\mathcal{H}(\mathbf{t}), \mathbf{y}_d)_H + \alpha s_{T_2}^T \mathbf{y}_d$  is an order  $\min(2q + 1, \rho)$  approximation of  $\mathcal{J}(\mathcal{Y}) = (\mathcal{H}(t), \mathcal{Y}) + \alpha \mathcal{Y}(T)$  for  $\mathcal{H}(t) \in C^\tau$ .*

*Proof.* The proof follows from Theorems 3 and 4.  $\square$

These last two theorems are the primary results of this section, showing that linear functionals of the solution integrated with the quadrature rule associated with the norm of GSBP operators are superconvergent and that the solution at block boundaries is also superconvergent. The additional flexibility of the generalized framework enables the construction of operators which are more efficient and are associated with more efficient quadrature rules. Thus, the evaluation of linear functionals and the solution at block boundaries from time-marching methods based on GSBP operators can be more efficient than those based on classical FD-SBP operators.



### 3.4. Stiff Source Terms

It is well known that implicit RK methods applied to problems with stiff source terms can suffer from what is called order reduction, where the convergence of the solution follows the accuracy of the internal stage approximations rather than the global order of the method. This is distinct from the case of stiff parasitic modes that might arise, for example, from semi-discrete approximations to PDEs and have negligible magnitude [39]. In that case, accuracy of these modes is not important, only their numerical stability.

A well-known investigation of stiff source terms and order reduction was carried out by Prothero and Robinson [49], who proposed the following problem to study stiff source terms

$$\mathcal{Y}' = \lambda\mathcal{Y} + \Psi' - \lambda\Psi, \quad (35)$$

where  $\Psi(t)$  is the prescribed exact solution, and  $\lambda \leq 0$  controls the stiffness of the source term. This is equivalent to the primal problem (10) with a stiff source term, and hence the stiffness comes from the homogeneous and particular solutions having different time scales. Numerical simulation [41, 47] indicates that similar order reduction is exhibited by classical FD-SBP-SAT discretizations, where the pointwise solution values can be considered analogous to the internal stage approximations of an RK method. This result is now extended for the GSBP-SAT approach, which in the stiff limit is described by the following theorem:

**Theorem 6.** *The pointwise accuracy of an order  $q$  GSBP-SAT discretization (11) of the linear IVP (10) with a stiff source term  $\mathcal{G}(t) = \Psi' - \lambda\Psi$  in the stiff limit is  $\frac{1}{\lambda}\mathcal{O}(q)$ .*

*Proof.* The proof follows analogously to Proposition 6 in [41]. □

This result supersedes the superconvergence of linear functionals and the numerical solution at block boundaries shown in Section 3.3. Therefore, in the case of stiff source terms the efficiency of the GSBP operator becomes more important than the efficiency of the associated quadrature rule. The order of dense-norm GSBP operators is less restricted by the order of the

associated quadrature rule than diagonal-norm GSBP operators. Hence, for certain quadrature rules the dense-norm GSBP operators can be more efficient for this class of problems relative to diagonal-norm GSBP operators with the same quadrature rule. The only caveat is the difference in nonlinear stability shown in Section 4.2.

## 4. Stability

Thus far it has been shown that the extensions of the generalized framework enable the construction of more efficient time-marching methods than those based on classical FD-SBP theory. These methods are only desirable for stiff IVPs if they also maintain the same stability properties. In this section, several linear and nonlinear stability criteria are considered. The analysis of these criteria for time-marching methods based on classical FD-SBP-SAT discretizations was done in [41] and does not rely on the existence of an internal stencil, nor a uniform nodal distribution. Hence, what remains to be shown is the extension for time-marching methods based on GSBP operators which do not include one or both boundary points.

### 4.1. Linear Stability

To begin the discussion of stability, consider the simplest IVP for a scalar autonomous linear ODE,

$$\mathcal{Y}' = \lambda \mathcal{Y}, \quad \mathcal{Y}(T_1) = f_{T_1}, \quad \text{with } T_1 \leq t \leq T_2, \quad (36)$$

where  $\mathcal{Y} \in \mathbb{C}$  and  $\lambda$  is a complex constant. It is well known that this equation, which is used for investigating the linear stability of time-marching methods, is inherently stable for  $\text{Re}(\lambda) \leq 0$  (*e.g.* [13, 39]). This can also be shown using the energy method [41].

In the discrete case,

$$D\mathbf{y}_d = \lambda \mathbf{y}_d + \sigma H^{-1} s_{T_1} (s_{T_1}^T \mathbf{y}_d - f_{T_1}), \quad (37)$$

unconditional stability of the numerical solution to the linear IVP (36) is

defined as A-stability [13]. A numerical method applied to (36) is called A-stable if  $\text{Re}(\lambda) \leq 0$  implies that

$$|\tilde{y}_{T_2}| \leq |f_{T_1}|, \quad (38)$$

where  $\tilde{y}_{T_2} \approx \mathcal{Y}(T_2)$ , is the numerical solution at time  $T_2$ , and  $f_{T_1}$  is the initial condition.

**Theorem 7.** *All dual-consistent GSBP-SAT discretizations (37) of the linear IVP (36) with  $\lambda \leq 0$  are A-stable.*

*Proof.* The proof is analogous to Proposition 1 in [41] using the ideas of [15] with  $\tilde{y}_{T_2} = s_{T_2}^T \mathbf{y}_d$ , rather than  $\mathbf{y}_{d,n}$ .  $\square$

This result guarantees that all linear scalar IVPs integrated with a time-marching method based on GSBP operators is always stable. However, A-stability is not necessarily optimal in all cases, as stiff components of the solution may be damped very slowly. This motivates an extension to the definition of A-stability, called L-stability [20]. A numerical method applied to (36) is called L-stable if it is A-stable, and furthermore  $\text{Re}(\lambda) \leq 0$  implies that

$$|\tilde{y}_{T_2}| \rightarrow 0 \text{ as } |\lambda| \rightarrow \infty. \quad (39)$$

Here, an alternate approach to [41] is given for the proof of L-stability, which is inspired by Proposition 3.8 in [26]. The proof is simplified by first introducing the following lemma:

**Lemma 2.** *If an extension of Assumption 1 from [41] holds for GSBP operators, then  $(\Theta + s_{T_1} s_{T_1}^T)^{-1} s_{T_1} = \mathbf{1}$ .*

*Proof.* Beginning with the assertion that  $(\Theta - \sigma s_{T_1} s_{T_1}^T)^{-1} s_{T_1} = \mathbf{1}$ , inserting the dual-consistent SAT penalty value  $\sigma = -1$ , multiplying through by  $(\Theta + s_{T_1} s_{T_1}^T)$ , and simplifying yields

$$s_{T_1} = (\Theta + s_{T_1} s_{T_1}^T) \mathbf{1} = \Theta \mathbf{1} + s_{T_1} s_{T_1}^T \mathbf{1}. \quad (40)$$

A consistent GSBP operator satisfies the identities  $D\mathbf{1} = \Theta\mathbf{1} = \mathbf{0}$  and  $s_{T_1}^T \mathbf{1} = 1$ , eliminating the first term on right side of the expression above and reducing the second term to  $s_{T_1}$ . This leads to an identity, proving the lemma.  $\square$

The proof is now presented for the L-stability of dual-consistent time-marching methods based on GSBP operators:

**Theorem 8.** *If an extension of Assumption 1 from [41] holds for GSBP operators, then all dual-consistent GSBP-SAT discretizations (37) of the linear IVP (36) with  $\text{Re}(\lambda) \leq 0$  are L-stable.*

*Proof.* The first requirement of L-stability, A-stability, follows from Theorem 7. For the additional requirement that  $|\tilde{y}_{T_2}| \rightarrow 0$  as  $|\lambda| \rightarrow \infty$ , consider the GSBP-SAT discretization (37) of (36). Rearranging using the extension of Assumption 1 from [41] and Lemma 2 yields

$$\begin{aligned} \mathbf{y}_d &= (\Theta + s_{T_1} s_{T_1}^T)^{-1} H \lambda \mathbf{y}_d + \mathbf{1} f_{T_1} \\ &= [I - \lambda(\Theta + s_{T_1} s_{T_1}^T)^{-1} H]^{-1} \mathbf{1} f_{T_1}, \end{aligned} \quad (41)$$

which can also be used to obtain an expression for  $\tilde{y}_{T_2}$

$$\tilde{y}_{T_2} = s_{T_2}^T \mathbf{y}_d = s_{T_2}^T (\Theta + s_{T_1} s_{T_1}^T)^{-1} H \lambda \mathbf{y}_d + s_{T_2}^T \mathbf{1} f_{T_1}. \quad (42)$$

Inserting (41) into (42), and recalling that  $s_{T_2}^T \mathbf{1} = 1$  for all GSBP operators yields

$$\tilde{y}_{T_2} = (1 + \lambda s_{T_2}^T (\Theta + s_{T_1} s_{T_1}^T)^{-1} H [I - \lambda(\Theta + s_{T_1} s_{T_1}^T)^{-1} H]^{-1} \mathbf{1}) f_{T_1}. \quad (43)$$

Taking the limit as  $|\lambda| \rightarrow \infty$

$$\tilde{y}_{T_2} = (1 - s_{T_2}^T (\Theta + s_{T_1} s_{T_1}^T)^{-1} H [(\Theta + s_{T_1} s_{T_1}^T)^{-1} H]^{-1} \mathbf{1}) f_{T_1}. \quad (44)$$

and simplifying yields

$$\tilde{y}_{T_2} = (1 - s_{T_2}^T \mathbf{1}) f_{T_1} = 0. \quad (45)$$

This implies that  $|\tilde{y}_{T_2}| \rightarrow 0$  as  $|\lambda| \rightarrow \infty$  and completes the proof.  $\square$

In addition to unconditional stability of scalar linear IVPs, this guarantees damping of stiff modes. Moving beyond scalar equations, a further stability definition, called linear stability, was proposed in [41] for linear systems of ordinary differential equations

$$\mathcal{Y}' = A\mathcal{Y}, \quad \mathcal{Y}(T_1) = f_{T_1}, \quad \text{with } T_1 \leq t \leq T_2, \quad (46)$$

where  $\mathcal{Y} \in \mathbb{C}^M$ , and  $A$  is an  $M \times M$  matrix. A numerical method applied to (46), for example obtained with a GSBP-SAT discretization,

$$(D \otimes I_M)\mathbf{y}_d = (I_n \otimes A)\mathbf{y}_d - \sigma(H^{-1}s_{T_1} \otimes I_M)((s_{T_1}^T \otimes I_M)\mathbf{y}_d - (I_n \otimes f_{T_1})), \quad (47)$$

is called linearly stable if  $PA + A^T P$  non-negative definite implies that

$$|\tilde{y}_{T_2}| \leq |f_{T_1}|, \quad (48)$$

where  $P$  is an SPD matrix defining a discrete inner product and norm over  $\mathbb{C}^M$ :

$$(\mathcal{Y}, \mathcal{Z})_P = \mathcal{Y}^* P \mathcal{Z}, \quad \|\mathcal{Y}\|_P^2 = \mathcal{Y}^* P \mathcal{Y}. \quad (49)$$

**Theorem 9.** *All dual-consistent GSBP-SAT discretizations (47) of the linear system of IVP (46) with  $PA + A^T P \geq 0$  are linearly stable.*

*Proof.* The proof is analogous to Proposition 2 in [41] using the ideas of [15] with  $\tilde{y}_{T_2} = s_{T_2}^T \mathbf{y}_d$ , rather than  $\mathbf{y}_{d,n}$ .  $\square$

In summary, all dual-consistent time-marching methods based on GSBP operators are unconditionally stable for linear problems, and furthermore provide damping of stiff modes. These conditions are derived for linear problems, but are often sufficient for nonlinear problems as well.

#### 4.2. Nonlinear Stability and Contractivity

Next, consider a subset of the general IVP (1) which satisfy the one-sided Lipschitz condition [14]:

$$\operatorname{Re}[(\mathcal{F}(\mathcal{Y}, t) - \mathcal{F}(\mathcal{Z}, t), \mathcal{Y} - \mathcal{Z})_P] \leq \nu \|\mathcal{Y} - \mathcal{Z}\|^2, \quad \forall \mathcal{Y}, \mathcal{Z} \in \mathbb{C}^M, \text{ and } t \in \mathbb{R} \quad (50)$$

where  $\nu \in \mathbb{R}$  is the one-sided Lipschitz constant, and  $P$  is an SPD matrix defining a discrete inner product and norm as in (49).

An IVP (1) is said to be contractive if it satisfies the one-sided Lipschitz condition with  $\nu \leq 0$ . The significance of this condition is that the distance between any two solutions,  $\|\mathcal{Y}(t) - \mathcal{Z}(t)\|$ , does not increase with time [26].

In the discrete case, it is desirable for the numerical method to behave in a similar fashion for contractive problems. This motivates the following definitions of B-stability [8] and BN-stability [6]. A numerical method applied to the autonomous form of (1) is called B-stable if the one-sided Lipschitz condition (50) with  $\nu \leq 0$  implies that

$$\|\tilde{y}_{T_2} - \tilde{z}_{T_2}\|_P \leq \|f_{T_1} - g_{T_1}\|_P, \quad (51)$$

where  $\tilde{y}_{T_2}$  and  $\tilde{z}_{T_2}$  are the numerical solutions at time  $T_2$  given initial data  $f_{T_1}$  and  $g_{T_1}$  respectively. A numerical method is called BN-stable if the same condition holds for the non-autonomous form of (1)<sup>1</sup>. Clearly BN-stability implies B-stability. In [41] it was shown that all dual-consistent time-marching methods based on diagonal-norm FD-SBP operators are BN-stable; however, the result does not hold for those based on dense-norm FD-SBP operators. This theory extends naturally for time-marching methods based on GSBP operators:

---

<sup>1</sup>BN-stability is sometimes referred to as B-stability when the distinction between autonomous and non-autonomous ODEs is not made (Compare Definitions 2.9.2 and 2.9.3 of [34] and Definition 12.2 in [26]).

**Theorem 10.** *All diagonal-norm dual-consistent GSBP-SAT discretizations (7) of the general IVP (1) which satisfy the Lipschitz condition (50) with  $\nu \leq 0$  are BN-stable and hence B-stable.*

*Proof.* The proof is analogous to Proposition 4 in [41] using the ideas of [15] with  $\tilde{y}_{T_2} = s_{T_2}^T \mathbf{y}_d$ , rather than  $\mathbf{y}_{d,n}$ .  $\square$

This implies that time-marching methods based on GSBP operators are unconditionally stable for nonlinear problems which are contractive. A similar nonlinear stability definition was presented in [7] for autonomous IVPs with monotonic functions. An extension of this idea for non-autonomous IVPs was introduced in [41], called energy stability. A numerical method is called energy stable if

$$\operatorname{Re}[(\mathcal{Y}(t), \mathcal{F}(\mathcal{Y}, t))_P] \geq 0, \quad \forall \mathcal{Y} \in \mathbb{C}^M, \text{ and } t \in \mathbb{R} \quad (52)$$

implies that

$$\|\tilde{y}_{T_2}\|_P \leq \|f_{T_1}\|_P. \quad (53)$$

This property is held by dual-consistent time-marching methods based on classical diagonal-norm FD-SBP operators, and extends for those based on diagonal-norm GSBP operators:

**Theorem 11.** *All diagonal-norm dual-consistent GSBP-SAT discretizations (7) of the general IVP (1) which satisfy (52) are energy stable, and hence monotonic.*

*Proof.* The proof is analogous to Proposition 3 in [41] using the ideas of [15] with  $\tilde{y}_{T_2} = s_{T_2}^T \mathbf{y}_d$ , rather than  $\mathbf{y}_{d,n}$ .  $\square$

In summary, in addition to the linear stability of all dual-consistent time-marching method based on GSBP operators, those associated with a diagonal norm satisfy the nonlinear stability criteria of energy stability and BN-stability as well.

## 5. Multistage approach

Thus far our analysis has assumed a global discretization of the problem in time. As discussed in the introduction, this can be prohibitively expensive and it may be advantageous to employ a multi-block implementation. This is analogous to a one-step multistage method like a RK scheme. This approach may also be necessitated for GSBP-SAT discretizations, as the operators can be of fixed size (no repeating internal stencil). In this section, we will show that the stability theorems of Section 4 extend to the multi-block case. In particular, we seek the conditions on the interface SAT penalty parameters of adjoining elements. This is an extension of the theory original developed in [12]. We will also investigate the change in pointwise order of accuracy when a multi-element approach is used in which the operators have a fixed size and temporal refinement is obtained by adding additional identical blocks rather than additional nodes within pre-existing blocks.

For the discussion of stability, consider a two-block GSBP-SAT discretization of the linear IVP (36):

$$\begin{aligned} \bar{H}^{-1} \begin{bmatrix} \Theta_L & 0 \\ 0 & \Theta_R \end{bmatrix} \mathbf{Y}_d = \lambda \mathbf{Y}_d + \bar{H}^{-1} \begin{bmatrix} \sigma_L s_{L\delta} s_{L\delta}^T & -\sigma_L s_{L\delta} s_{R\delta}^T \\ -\sigma_R s_{R\delta} s_{L\delta}^T & \sigma_R s_{R\delta} s_{R\delta}^T \end{bmatrix} \mathbf{Y}_d \\ + \sigma H_L^{-1} s_{T_1} (s_{T_1}^T \mathbf{y}_{d,L} - f_{T_1}), \end{aligned} \quad (54)$$

where the composite norm and solution are defined as

$$\bar{H} = \begin{bmatrix} H_L & 0 \\ 0 & H_R \end{bmatrix}, \quad \text{and} \quad \mathbf{Y}_d = \begin{bmatrix} \mathbf{y}_{d,L} \\ \mathbf{y}_{d,R} \end{bmatrix}, \quad (55)$$

and the elements of the left and right blocks are  $\mathbf{y}_{d,L}$  in  $[T_1, \delta]$  and  $\mathbf{y}_{d,R}$  in  $[\delta, T_2]$  respectively, with their interface at  $T_1 \leq \delta \leq T_2$ . Applying the energy method, simplifying, and rearranging leads to

$$\begin{aligned} |\tilde{y}_{R,T_2}|^2 = 2\text{Re}(\lambda) \|\mathbf{Y}_d\|_{\bar{H}}^2 + (1 + 2\sigma) \left| \tilde{y}_{L,T_1} - \frac{\sigma}{1+2\sigma} f_{T_1} \right|^2 - \frac{\sigma^2}{1+2\sigma} |f_{T_1}|^2 \\ + \mathbf{Y}_d^* \begin{bmatrix} (-1 + 2\sigma_L) s_{L\delta} s_{L\delta}^T & -(\sigma_L + \sigma_R) s_{L\delta} s_{R\delta}^T \\ -(\sigma_R + \sigma_L) s_{R\delta} s_{L\delta}^T & (1 + 2\sigma_R) s_{R\delta} s_{R\delta}^T \end{bmatrix} \mathbf{Y}_d, \end{aligned} \quad (56)$$



which bounds the numerical solution at time  $T_2$  by the initial data, in the sense that  $|\tilde{y}_{R,T_2}|^2 \leq K|f_{T_1}|^2$  with  $K$  is a positive real number, provided that  $\text{Re}(\lambda) \leq 0$ ,  $\sigma < -\frac{1}{2}$ , and the matrix in the last term is negative semi-definite. This will occur if

$$\sigma_L = \sigma_R + 1, \quad \text{and} \quad \sigma_R \leq -\frac{1}{2}. \quad (57)$$

This relationship between the SAT parameters of the right and left block is identical to the result obtained in [12] for the classical FD-SBP-SAT approach. Furthermore, if  $\sigma_R$  is chosen to be  $-1$ , then the solution in the left block becomes independent of the solution in the right block. Again, this is equivalent to the result for multi-block FD-SBP-SAT discretizations shown in [41]. As a consequence, the block solutions can be computed sequentially in time rather than fully coupled. With the choice of  $\sigma = \sigma_R = -1$ , the energy estimate becomes

$$|\tilde{y}_{R,T_2}|^2 = 2\text{Re}(\lambda) \|\mathbf{Y}_d\|_{\tilde{H}}^2 - |\tilde{y}_{L,T_1} - f_{T_1}|^2 - |\tilde{y}_{R,\delta} - \tilde{y}_{L,\delta}|^2 + |f_{T_1}|^2, \quad (58)$$

and the method is A-stable:

$$|\tilde{y}_{R,T_2}|^2 \leq |f_{T_1}|^2, \quad (59)$$

This procedure can be repeated to extend the other linear and nonlinear stability results of Section 4.

Next, we consider the accuracy of the multi-element approach for the primal and dual problems. This divides the problem into two time scales: one associated with the number of elements in the discretization, the other with the subdiscretization within the element. This is exploited to show that the pointwise accuracy of the multi-element approach is one order higher than shown for the general case in Theorems 1 and 2. Note that this does not supersede the expected order of convergence for problems with stiff source terms presented in Theorem 6. The theorems are now stated:

**Theorem 12.** *The pointwise accuracy of a multi-element GSBP-SAT discretization (11) of the primal problem (10) with  $\text{Re}(\lambda) \leq 0$  using GSBP operators of fixed size  $n$  and order  $q$ , along with a compatible SAT implementation, is of order  $q + 1$  provided an extension of Assumption 2 from [41] holds for GSBP operators.*

*Proof.* Define two time scales: 1) the elemental time scale  $\Delta t_N = \frac{T_2 - T_1}{N}$ , where  $N$  is the number of elements in the discretization; and 2) the nodal time scale  $\Delta t_n = \frac{\Delta t_N}{n}$ , which also relates the two time scales.

From Theorem 1 we know that the accuracy of the solution within each element is of order  $\mathcal{O}(\Delta t_n^q)$ . However, the contribution from each element is now of order  $\Delta t_N$ , rather than  $T_2 - T_1 = \mathcal{O}(1)$ . Thus the order of the the multi-element approximation is  $\mathcal{O}(\Delta t_N)\mathcal{O}(\Delta t_n^q)$ . Using the relationship between the two time scales yields the order of the pointwise accuracy:

$$\begin{aligned} \mathcal{O}(\Delta t_N)\mathcal{O}(\Delta t_n^q) &= \mathcal{O}(\Delta t_N)\mathcal{O}\left(\frac{1}{n^q}\Delta t_N^q\right) \\ &= \mathcal{O}(\Delta t_N^{q+1}), \end{aligned} \tag{60}$$

thus completing the proof.  $\square$

**Theorem 13.** *The pointwise accuracy of a dual-consistent multi-element GSBP-SAT discretization (21) of the continuous dual problem (14) using GSBP operators of fixed size  $n$  and order  $q$ , along with a compatible SAT implementation, is of order  $q + 1$  provided an extension of Assumption 2 from [41] holds for GSBP operators.*

*Proof.* The proof follows from Theorems 12 and 2.  $\square$

These theorems show that using a multi-element approach, one is guaranteed an additional order of pointwise accuracy over the general case. However, in practice this additional order of accuracy is seen even when a multi-element approach is not used.

## 6. Numerical Examples

This section presents numerical solutions to two simple model problems with the purpose of demonstrating some of the theory presented in this article

| SBP Scheme                                     | Norm       | Abbr. | $q$                         | $\tau$                       | L/B-stable |
|------------------------------------------------|------------|-------|-----------------------------|------------------------------|------------|
| Classical Finite-Difference<br>→ Element-Based | Diag. [38] | CME   | $\frac{n}{4}$               | $\frac{n}{2}$                | Y / Y      |
|                                                | Block [51] | CMEB  | $\frac{n}{2} - 1$           | $\frac{n}{2}$                | Y / N      |
| Newton-Cotes                                   | Diag. [15] | NC    | $\lceil \frac{n}{2} \rceil$ | $2\lceil \frac{n}{2} \rceil$ | Y / Y      |
|                                                | Dense [10] | NCB   | $n$                         | $2\lceil \frac{n}{2} \rceil$ | Y / N      |
| Legendre-Gauss-Lobatto                         | Diag. [23] | LGL   | $n$                         | $2n - 2$                     | Y / Y      |
| Legendre-Gauss-Lobatto                         | Dense [10] | LGLB  | $n$                         | $2n - 2$                     | Y / N      |
| Legendre-Gauss-Radau                           | Diag. [15] | LGR   | $n$                         | $2n - 1$                     | Y / Y      |
| Legendre-Gauss                                 | Diag. [15] | LG    | $n$                         | $2n$                         | Y / Y      |

Table 2: Summary of SBP operators, their associated abbreviations and general properties. Notes: 1) the general properties of diagonal-norm SBP operators based on Newton-Cotes quadrature hold only for the case of positive quadrature weights; 2) the value for  $q$  given for CME applies only to  $q \geq 2$ .

and providing an initial characterization of time-marching methods based on classical FD-SBP and GSBP operators for IVPs. A summary of the GSBP time-marching methods investigated is presented in Table 2 along with their associated properties and abbreviations used hereafter. This includes the classical FD-SBP operators which are a subset of GSBP operators. More details on the non-classical GSBP operators can be found in [15].

### 6.1. Prothero-Robinson problem

Here the Prothero-Robinson problem (35) is solved with exact solution  $\Psi(t) = e^{-t}$ , equivalent to the primal problem (10) with a source term  $\mathcal{G}(t) = -(1 + \lambda)e^{-t}$ . The intent is to compare the convergence rates of the GSBP time-marching methods for problems with stiff and non-stiff source terms. The stiffness of the problem is controlled via the parameter  $\lambda$ . The choice of  $\lambda = -2$  is selected for a non-stiff source term, and  $\lambda = -1000$  for a stiff source term [41, 47]. Note that all GSBP time-marching methods are implemented with dual-consistent SAT penalty values.

The primary results are convergence rates are based on two error measures: 1) the solution error at the nodal locations:

$$e_{y_i} = \|\mathbf{y}_d - \mathbf{y}\|_{\bar{H}} = \sqrt{(\mathbf{y}_d - \mathbf{y})^T \bar{H} (\mathbf{y}_d - \mathbf{y})}, \quad (61)$$

where  $\bar{H}$  is a composite norm consistent with the GSBP time-marching method; 2) the discrete L2 norm of the solution at each element boundary:

$$e_{y_e} = \sqrt{\frac{\sum_{j=1}^N (s_{T_2}^T \mathbf{y}_{d,j} - \mathcal{Y}(j\Delta t))^2}{N}}, \quad (62)$$

where  $N$  represents the number of elements in the discretization.

#### 6.1.1. Accuracy of problems with a non-stiff source term ( $\lambda = -2$ )

Table 3 summarizes the convergence rates of the Prothero-Robinson problem with a non-stiff source term. The results for time-marching methods based on classical FD-SBP operators are obtained with minimum block size operators in a multi-element implementation. This has been shown to have similar accuracy to the global approach [41]. The convergence of the pointwise solution error  $e_{y_i}$  is order  $q + 1$  for both time-marching methods based on classical FD-SBP and GSBP operators, where  $q$  is the minimum global pointwise order of the scheme. This is in line with Theorem 12 and what has been observed in [15, 41, 47].

The table highlights the relatively small number of nodes required by time-marching methods based on GSBP operators to achieve the same order of accuracy as those based on classical FD-SBP operators. This is seen even in the case of the diagonal-norm NC GSBP operators, the accuracy of which is limited to  $q = \lfloor \frac{\tau}{2} \rfloor \leq n - 1$ . In all the other cases for both diagonal and dense-norm GSBP operators, the order of the operator is limited to  $q = n - 1$  independent of the order of the associated quadrature.

If one considers only the solution at the element boundaries  $e_{y_e}$ , the convergence of GSBP time-marching methods is of order  $\min(2q + 1, \rho)$ , where  $\rho$  is the order of the associated norm. This is in line with Theorem 5 for dual-consistent discretizations, which implies that the solution at the element boundaries is superconvergent.

| SBP<br>Scheme | $q = 1$ |        |                   | $q = 2$ |        |                   | $q = 3$ |        |                   | $q = 4$ |        |                   |
|---------------|---------|--------|-------------------|---------|--------|-------------------|---------|--------|-------------------|---------|--------|-------------------|
|               | $n$     | $\tau$ | $p_{y_i}/p_{y_e}$ | $n$     | $\tau$ | $p_{y_i}/p_{y_e}$ | $n$     | $\tau$ | $p_{y_i}/p_{y_e}$ | $n$     | $\tau$ | $p_{y_i}/p_{y_e}$ |
| CME           | 2       | 2      | 1.9842 / 1.9699   | 8       | 4      | 2.9603 / 3.9911   | 12      | 6      | 3.9130 / 5.9730   | 16      | 8      | 4.8452 / -        |
| CMEB          | 2       | 2      | 1.9842 / 1.9699   | -       | -      | -                 | 8       | 4      | 3.9725 / 3.9927   | -       | -      | -                 |
| NC            | 2       | 2      | 1.9878 / 1.9767   | 3       | 4      | 2.9916 / 3.9817   | 5       | 6      | 3.8428 / 5.9630   | 7       | 8      | 4.9552 / 7.8919   |
| NCB           | 2       | 2      | 1.9965 / 1.9856   | 3       | 4      | 2.9925 / 3.9733   | 4       | 4      | 3.9928 / 3.9973   | 5       | 6      | 4.9832 / 5.9958   |
| LGL           | 2       | 2      | 1.9878 / 1.9767   | 3       | 4      | 2.9916 / 3.9817   | 4       | 6      | 3.9761 / 5.9423   | 5       | 8      | 4.9451 / 7.8770   |
| LGLB          | 2       | 2      | 1.9965 / 1.9856   | 3       | 4      | 2.9925 / 3.9733   | 4       | 4      | 3.9816 / 5.9357   | 5       | 6      | 4.9589 / 7.8724   |
| LGR           | 2       | 3      | 1.9949 / 2.9901   | 3       | 5      | 2.9919 / 4.9825   | 4       | 7      | 3.9808 / 6.9472   | 5       | 9      | 4.9581 / 8.9119   |
| LG            | 2       | 4      | 1.9909 / 2.9892   | 3       | 6      | 2.9853 / 4.9784   | 4       | 8      | 3.9660 / 6.9676   | 5       | 10     | 4.9304 / 8.9109   |

Table 3: **Prothero-Robinson Problem** ( $\lambda = -2$ ): Convergence rates,  $p_{y_i}$  of the pointwise solution error,  $e_{y_i}$ , and  $p_{y_e}$  of the element boundary solution error,  $e_{y_e}$ . The order of the SBP operator is given by  $q$ ,  $n$  is the number of nodes in each element, and  $\tau$  is the order of the associated quadrature rule. The convergence rates were computed using a line of best fit.

| SBP<br>Scheme | $q = 1$ |        |                   | $q = 2$ |        |                   | $q = 3$ |        |                   | $q = 4$ |        |                   |
|---------------|---------|--------|-------------------|---------|--------|-------------------|---------|--------|-------------------|---------|--------|-------------------|
|               | $n$     | $\tau$ | $p_{y_i}/p_{y_e}$ | $n$     | $\tau$ | $p_{y_i}/p_{y_e}$ | $n$     | $\tau$ | $p_{y_i}/p_{y_e}$ | $n$     | $\tau$ | $p_{y_i}/p_{y_e}$ |
| CME           | 2       | 2      | 1.0404 / 0.9202   | 8       | 4      | 2.0252 / 2.0617   | 12      | 6      | 3.0770 / 3.1449   | 16      | 8      | 4.0328 / 4.1979   |
| CMEB          | 2       | 2      | 1.0404 / 0.9202   | -       | -      | -                 | 8       | 4      | 3.0627 / 3.1824   | -       | -      | -                 |
| NC            | 2       | 2      | 1.0181 / 0.9412   | 3       | 4      | 2.0003 / 1.9870   | 5       | 6      | 3.0497 / 3.0459   | 7       | 8      | 4.1544 / 4.2056   |
| NCB           | 2       | 2      | 1.0181 / 0.9412   | 3       | 4      | 2.0003 / 1.9870   | 4       | 4      | 3.0689 / 3.0312   | 5       | 6      | 4.0207 / 4.0899   |
| LGL           | 2       | 2      | 1.0181 / 0.9412   | 3       | 4      | 2.0003 / 1.9870   | 4       | 6      | 3.0433 / 3.0464   | 5       | 8      | 4.0129 / 4.1307   |
| LGLB          | 2       | 2      | 1.0553 / 0.9773   | 3       | 4      | 2.0044 / 1.9941   | 4       | 6      | 3.0965 / 3.1039   | 5       | 8      | 4.0312 / 4.1599   |
| LGR           | 2       | 3      | 1.0229 / 1.9911   | 3       | 5      | 2.0701 / 3.0036   | 4       | 7      | 3.1314 / 4.1111   | 5       | 9      | 4.1725 / 5.1658   |
| LG            | 2       | 4      | 0.9941 / 1.9768   | 3       | 6      | 2.0576 / 2.9939   | 4       | 8      | 3.1192 / 4.1038   | 5       | 10     | 4.1657 / 5.1599   |

Table 4: **Prothero-Robinson Problem** ( $\lambda = -1000$ ): Convergence rates,  $p_{y_i}$  of the pointwise solution error,  $e_{y_i}$ , and  $p_{y_e}$  of the element boundary solution error,  $e_{y_e}$ . The order of the SBP operator is given by  $q$ ,  $n$  is the number of nodes in each element, and  $\tau$  is the order of the associated quadrature rule. The convergence rates were computed using a line of best fit.

The table also confirms the relatively small number of nodes required by time-marching methods based on GSBP operators to achieve the same order of superconvergence of linear functionals as those based on classical FD-SBP operators. Furthermore, it shows the benefit of allowing the nodal distribution to be nonuniform in the computational domain. For example, the order of superconvergence,  $p_{ye}$ , exhibited by the operators associated with Legendre-Gauss-Lobatto quadrature rules increases about twice as fast with the number nodes as the operators associated with the Newton-Cotes quadrature rules. Also, there is a limit to the superconvergence as seen with the GSBP time-marching methods associated with Legendre-Gauss quadrature rules. Despite the associate quadrature being order  $2q + 2$ , the order of convergence of the boundary solutions is only  $2q + 1$  as per Theorem 5.

Figure 1 shows the relative magnitude of the solution error as a function of the number of degrees of freedom (DOFs). Results are presented for operators of order  $q = 3$  with the understanding that the conclusions equally apply to operators of other orders, especially as the order increases. Figure 1(a) shows that the relative magnitude of the pointwise solution error produced by operators is very similar. The difference exists when only the solution at element boundaries is considered, (see Figure 1(b)). In this case, the importance of the order of the associated norm is seen, as it dictates the maximum rate of superconvergence. In each case, the GSBP time-marching methods based on Legendre-Gauss-Radau and Legendre-Gauss quadrature rules have the lowest error with respect to DOFs. These schemes make use of all three extensions of the generalized framework. If one considers only operators whose nodal distribution includes the boundary points, the diagonal-norm NC, LGL and CME schemes perform similarly. However, this does not take into account the larger size of the CME operators, which reduces their efficiency relative to the other methods. In fact, nearly all the time-marching methods based on GSBP operators presented in this figure are half the size of the time-marching method based on the dense-norm classical FD-SBP operator and a third the size of the time-marching method based on the diagonal-norm classical FD-SBP operator.

### 6.1.2. Accuracy of problems with a stiff source term ( $\lambda = -1000$ )

Table 4 shows a similar summary of convergence rates for the Prothero-Robinson problem with a stiff source term ( $\lambda = -1000$ ). The convergence rates are taken from the stiff region of the convergence plots. As the num-

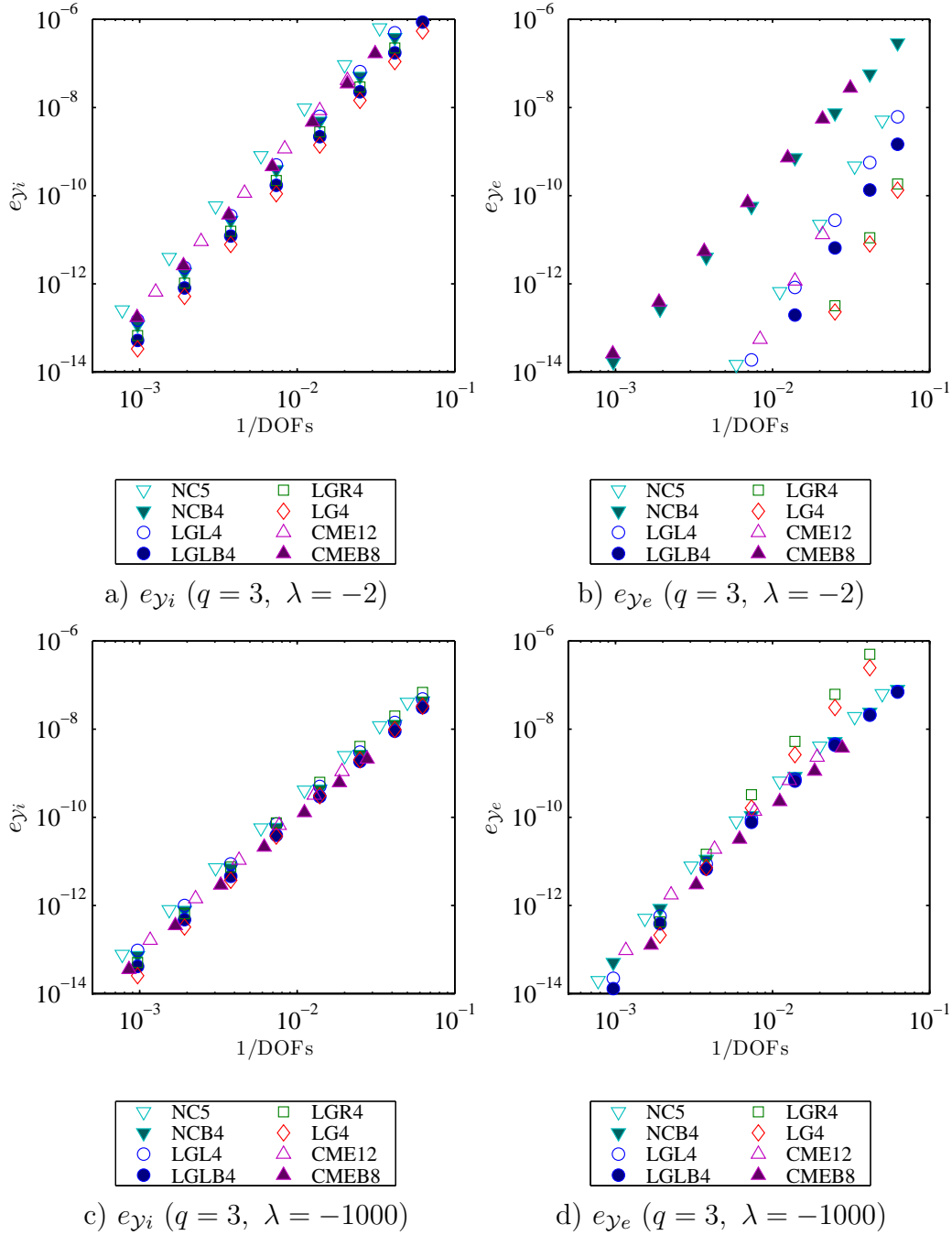


Figure 1: **Prothero-Robinson Problem:** Convergence of the pointwise solution,  $e_{\gamma_i}$ , and element boundary solution error,  $e_{\gamma_e}$  with respect to DOFs. The order of the SBP operator is given by  $q$ , and the subscript in the legend indicates the number of nodes in each element.

ber of DOFs is further increased, the stiff portion of solution begins to be adequately resolved, eliminating the stiffness. As predicted in Section 3.4, the convergence rate in the stiff region of both the pointwise solution and the element boundary solution error drops to order  $q$ . The exceptions are GSBP time-marching methods associated with the Legendre-Gauss-Radau and Legendre-Gauss quadrature rules, which achieve convergence of order  $q + 1$ .

The table highlights the benefit of the time-marching methods based on dense-norm CMEB and NCB operators over their diagonal-norm counterparts for problems with stiff source terms. The advantage of the dense-norm operators is that they achieve the same rate of convergence with fewer nodes in each element. This translates to reduced computational cost, and therefore increased efficiency.

Figure 1 also shows the relative magnitude of the solution error as a function of the number of DOFs for the Prothero-Robinson problem with a stiff source term ( $\lambda = -1000$ ). As with the non-stiff source term, the magnitude of the pointwise solution error is nearly identical for the various discretizations of order  $q$ . The difference is that this trend is also exhibited for the element boundary error. The only noticeable deviation is with the GSBP time-marching methods associated with Legendre-Gauss-Radau and Legendre-Gauss quadrature rules that have slightly higher error in the stiffest region of the convergence plots. However, the higher rate of convergence in this region means that the magnitude is quickly reduced with the increase of DOFs.

What is not seen directly from the table or figure is the stability of the approach. The numerical results with the stiff source term are all stable independent of the step size chosen, exemplifying the unconditional stability of the approach for linear problems.

### 6.2. Van der Pol's equation

Van der Pol's equation is a second-order nonlinear ODE

$$y'' - \mu(1 - y^2)y' + y = 0,$$

which we solve as a first-order system:



| SBP<br>Scheme | $q = 1$ |        |                                       | $q = 3$ |        |                                       | $q = 4$ |        |                                       |
|---------------|---------|--------|---------------------------------------|---------|--------|---------------------------------------|---------|--------|---------------------------------------|
|               | $n$     | $\tau$ | $p_{\mathcal{Y}_1}/p_{\mathcal{Y}_2}$ | $n$     | $\tau$ | $p_{\mathcal{Y}_1}/p_{\mathcal{Y}_2}$ | $n$     | $\tau$ | $p_{\mathcal{Y}_1}/p_{\mathcal{Y}_2}$ |
| CME           | 2       | 2      | 1.9129 / 1.9166                       | 12      | 6      | 5.9484 / 5.9547                       | 16      | 8      | 7.6569 / 7.5954                       |
| CME           | 2       | 2      | 1.9129 / 1.9166                       | 8       | 4      | 4.0028 / 3.9981                       | -       | -      | -                                     |
| NC            | 2       | 2      | 1.9129 / 1.9166                       | 5       | 6      | 5.9016 / 5.9043                       | 7       | 8      | 7.4841 / 7.4642                       |
| NCB           | 2       | 2      | 1.9401 / 2.2670                       | 4       | 4      | 5.8833 / 6.0321                       | 5       | 6      | 7.3746 / 7.6408                       |
| LGL           | 2       | 2      | 1.9129 / 1.9166                       | 4       | 6      | 5.8844 / 5.9263                       | 5       | 8      | 7.8354 / 7.8120                       |
| LGLB          | 2       | 2      | 1.9401 / 2.2670                       | 4       | 6      | 6.0184 / 6.1597                       | 5       | 8      | 7.7804 / 8.0606                       |
| LGR           | 2       | 3      | 2.9716 / 2.9724                       | 4       | 7      | 6.9013 / 6.9068                       | 5       | 9      | 8.6413 / 8.6240                       |
| LG            | 2       | 4      | 2.9708 / 2.9716                       | 4       | 8      | 6.8972 / 6.9027                       | 5       | 10     | 8.6109 / 8.5916                       |

Table 5: **Van der Pol's equation** ( $\mu = 10$ ): Convergence rates,  $p_{\mathcal{U}}$  of the pointwise solution error,  $e_{\mathcal{U}}$ , and  $p_{\mathcal{F}}$  of the element boundary solution error,  $e_{\mathcal{F}}$ . The order of the SBP operator is given by  $q$ ,  $n$  is the number of nodes in each element, and  $\tau$  is the order of the associated quadrature rule. The convergence rates were computed using a line of best fit.

$$\left\{ \begin{array}{l} y' = z \\ z' = \mu(1 - y^2)z - y \end{array} \right\},$$

where  $\mu$  is called the stiffness parameter. The initial conditions are  $y = 2$  and  $z = -0.6666654321121172$ , and the domain is  $t = [0, 0.5]$ [36]. The aim is to evaluate the performance of time-marching methods based on GSBP operators for nonlinear problems. A relatively small value of 10 is chosen for  $\mu$ , leading to a non-stiff problem. The error definitions used for the Prothero-Robinson problem are applied here to each component of the solution independently.

Table 5 summarizes the convergence of the GSBP time-marching methods for the nonlinear non-stiff van der Pol equation. A reduced set of results is presented, as they are very similar to the convergence rates for the linear Prothero-Robinson equation. The significance of this, is that the superconvergence result derived in Section 3.3 appears to hold for nonlinear problems as well. Indeed, if the operators are cast as RK methods, they satisfy the general order conditions for nonlinear problems up to the order predicted by Theorem 5. Proof of this will be presented in a future article.

## 7. Conclusions

This article extends the theory of generalized summation-by-parts operators and simultaneous approximation terms originally presented in [15] for application to initial-value problems. The generalized framework encompasses both classical finite-difference summation-by-parts operators as well as those that: 1) have no repeating internal stencil; 2) have nonuniform nodal distributions in the computational domain; and 3) have nodal distributions which do not include one or both boundary points. This enables the construction of more efficient SBP operators which can be used to increase the order of a simulation for a fixed computational cost or to reduce the number of solutions required to be fully coupled in time for a given order of accuracy. Therefore, high-order implicit time-marching methods based on GSBP operators can be more efficient than those based on classical FD-SBP operators.

Time-marching methods based on GSBP operators are shown to maintain the same stability and accuracy properties as those based on classical FD-SBP operators. Specifically, all dual-consistent time-marching methods based on GSBP operators are shown to be linearly stable, provide damping of stiff modes, and those constructed with a diagonal norm are shown to be nonlinearly stable as well. These results are shown to hold for multi-block discretizations with the appropriate choice of SAT values. The theory of superconvergent linear functionals is also extended to the generalized framework. It is shown that if the solution is dual-consistent and sufficiently smooth, then linear functionals integrated with the quadrature associated with the GSBP-SAT discretization are guaranteed to converge with the minimum of: 1) the minimum required order of the quadrature; and 2) one plus twice the order of the GSBP operator itself. This theory also implies that the solution at the element boundaries is superconvergent, analogous to a Runge-Kutta method with low stage order and higher-order solution update. Finally, the pointwise accuracy of the multi-element approach is shown to be superconvergent to the order of the discretization plus one.

Numerical simulations are presented to demonstrate the theoretical results of the article. Superconvergence of the solution at element boundaries is observed for the Prothero-Robinson problem with a non-stiff source term and order-reduction to the order of the individual operators with a stiff source term. Furthermore, solutions with a stiff source term remain stable indepen-

dent of the size of the time step, exemplifying the unconditional stability of the approach for linear problems. Lastly, numerical simulation of the non-stiff nonlinear van der Pol's equation exhibit the same superconvergence as the linear Prothero-Robinson problem with non-stiff source term. This demonstrates that some of the accuracy results generated for linear problems in this article can also hold for nonlinear problems.

### Acknowledgements

The authors gratefully acknowledge the financial assistance of the Ontario Graduate Scholarship program and the University of Toronto.

### References

- [1] S.S. Abarbanel, A.E. Chertock, Strict Stability of High-order Compact Implicit Finite-difference Schemes: The Role of Boundary Conditions for Hyperbolic PDEs, I, *J. Comput. Phys.* 160 (2000) 42–66.
- [2] S.S. Abarbanel, A.E. Chertock, A. Yefet, Strict Stability of High-order Compact Implicit Finite-difference Schemes: The Role of Boundary Conditions for Hyperbolic PDEs, II, *Journal of Computational Physics* 160 (2000) 67–87.
- [3] S.S. Abarbanel, A. Ditkowski, Multi-dimensional asymptotically stable 4th-order accurate schemes for the diffusion equation, Technical Report, 1996.
- [4] S.S. Abarbanel, A. Ditkowski, Asymptotically Stable Fourth-order Accurate Schemes for the Diffusion Equation on Complex Shapes, *J. Comput. Phys.* 133 (1997) 279–288.
- [5] J. Berg, J. Nordström, Superconvergent Functional Output for Time-dependent Problems Using Finite Differences on Summation-by-parts Form, *J. Comput. Phys.* 231 (2012) 6846–6860.
- [6] K. Burrage, J.C. Butcher, Stability Criteria for Implicit Runge-Kutta Methods, *SIAM Journal on Numerical Analysis* 16 (1979) pp. 46–57.
- [7] K. Burrage, J.C. Butcher, Non-linear Stability of a General Class of Differential Equation Methods, *BIT Numerische Mathematik* 20 (1980) 185–203.

- [8] J. Butcher, A stability property of implicit Runge-Kutta methods, *BIT Numerical Mathematics* 15 (1975) 358–361.
- [9] M.H. Carpenter, T.C. Fisher, N.K. Yamaleev, Boundary Closures for Sixth-Order Energy-Stable Weighted Essentially Non-Oscillatory Finite-Difference Schemes, in: *Advances in Applied Mathematics, Modeling, and Computational Science*, Volume 66 of *Fields Institute Communications*, Springer US, 2013, pp. 117–160.
- [10] M.H. Carpenter, D. Gottlieb, Spectral methods on arbitrary grids, *Journal of Computational Physics* 129 (1996) 74–86.
- [11] M.H. Carpenter, D. Gottlieb, S.S. Abarbanel, Time-stable boundary conditions for finite-difference schemes solving hyperbolic systems: methodology and application to high-order compact schemes, *Journal of Computational Physics* 111 (1994) 220–236.
- [12] M.H. Carpenter, J. Nordström, D. Gottlieb, A stable and conservative interface treatment of arbitrary spatial accuracy, *Journal of Computational Physics* 148 (1999) 341–365.
- [13] G.G. Dahlquist, A special stability problem for linear multistep methods, *BIT Numerical Mathematics* 3 (1963) 27–43.
- [14] K. Dekker, J. Verwer, *Stability of Runge-Kutta methods for stiff nonlinear differential equations*, CWI monograph, 1984.
- [15] D.C. Del Rey Fernández, P.D. Boom, D.W. Zingg, A Generalized Framework for Nodal First Derivative Summation-By-Parts Operators, *Journal of Computational Physics* 266 (2014) 214–239.
- [16] D.C. Del Rey Fernández, J.E. Hicken, D.W. Zingg, Review of Summation-By-Parts Operators with Simultaneous Approximation Terms for the Numerical Solution of Partial Differential Equations, *Computers & Fluids* 95 (2014) 171–196.
- [17] D.C. Del Rey Fernández, D.W. Zingg, High-order compact-stencil summation-by-parts operators for the second derivative with variable coefficients, *ICCFD7-2803* (2012).

- [18] D.C. Del Rey Fernández, D.W. Zingg, Generalized Summation-By-Parts Operators for the Second Derivative with Constant or Variable Coefficients, *Journal of Computational Physics* (2014). (submitted).
- [19] A. Ditkowski, Bounded-Error Finite Difference Schemes for Initial Boundary Value Problems on Complex Domains, Ph.D. thesis, Tel-Aviv University, 1997.
- [20] B.L. Ehle, On Padé approximations to the exponential function and A-stable methods for the numerical solution of initial value problems, Technical Report CS-RR-2010, Dept. AACS, University of Waterloo, 1969.
- [21] D. Funaro, D. Gottlieb, A new method of imposing boundary conditions in pseudospectral approximations of hyperbolic equations, *Mathematics of Computation* 51 (1988) 599–613.
- [22] D. Funaro, D. Gottlieb, Convergence Results for Pseudospectral Approximations of Hyperbolic Systems by a Penalty-Type Boundary Treatment, *Mathematics of Computation* 57 (1991) 585–596.
- [23] G.J. Gassner, A skew-symmetric discontinuous Galerkin spectral element discretization and its relation to SBP-SAT finite difference methods, *SIAM Journal on Scientific Computing* 35 (2013).
- [24] B. Gustafsson, *High Order Difference Methods for Time Dependent PDE*, Springer, 2008.
- [25] B. Gustafsson, H.O. Kreiss, J. Olinger, *Time Dependent Problems and Difference Methods*, Wiley-Interscience, 1996.
- [26] E. Hairer, G. Wanner, *Solving Ordinary Differential Equations II*, Springer, Berlin, 1991.
- [27] J.S. Hesthaven, A stable penalty method for the compressible Navier-Stokes equations: II. One-dimensional domain decomposition schemes, *SIAM Journal on Scientific Computing* 18 (1997) 658–685.
- [28] J.S. Hesthaven, A Stable Penalty Method for the Compressible Navier–Stokes Equations: III. Multidimensional Domain Decomposition Schemes, *SIAM J. Sci. Comput.* 20 (1998) 62–93.

- [29] J.S. Hesthaven, D. Gottlieb, A Stable Penalty Method for the Compressible Navier–Stokes Equations: I. Open Boundary Conditions, *SIAM J. Sci. Comput.* 17 (1996) 579–612.
- [30] J.E. Hicken, D.W. Zingg, A parallel Newton-Krylov solver for the Euler equations discretized using simultaneous approximation terms, *AIAA Journal* 46 (2008) 2773–2786.
- [31] J.E. Hicken, D.W. Zingg, Superconvergent Functional Estimates from Summation-By-Parts Finite-Difference Discretizations, *SIAM J. Sci. Comput.* 33 (2011) 893–922.
- [32] J.E. Hicken, D.W. Zingg, Summation-By-Parts Operators and High-Order Quadrature, *Journal of Computational and Applied Mathematics* 237 (2013) 111–125.
- [33] J.E. Hicken, D.W. Zingg, Dual Consistency and Functional Accuracy: A Finite-difference Perspective, *J. Comput. Phys.* 256 (2014) 161–182.
- [34] Z. Jackiewicz, *General Linear Methods for Ordinary Differential Equations*, Wiley, 2009.
- [35] R. Kamakoti, C. Pantano, High-order narrow stencil finite-difference approximations of second-derivatives involving variable coefficients, *SIAM Journal on Scientific Computing* 31 (2009) 4222–4243.
- [36] C.A. Kennedy, M.H. Carpenter, Additive Runge-Kutta Schemes for Convection-diffusion-reaction Equations, *Appl. Numer. Math.* 44 (2003) 139–181.
- [37] H.O. Kreiss, J. Lorenz, Initial-Boundary Value Problems and the Navier-Stokes Equations, Volume 47 of *Classics in Applied Mathematics*, SIAM, 2004.
- [38] H.O. Kreiss, G. Scherer, Finite element and finite difference methods for hyperbolic partial differential equations, in: *Mathematical aspects of finite elements in partial differential equations*, Academic Press, New York/London, 1974, pp. 195–212.
- [39] H. Lomax, T.H. Pulliam, D.W. Zingg, *Fundamentals of Computational Fluid Dynamics*, Scientific Computation, Springer, 2001.

- [40] J. Lu, An *a posteriori* Error Control Framework for Adaptive Precision Optimization using Discontinuous Galerkin Finite Element Method, Ph.D. thesis, Massachusetts Institute of Technology, 2005.
- [41] T. Lundquist, J. Nordström, The SBP-SAT Technique for Initial Value Problems, *Journal of Computational Physics* 270 (2014) 86–104.
- [42] K. Mattsson, Summation by Parts Operators for Finite Difference Approximations of Second-Derivatives with Variable Coefficients, *J. Sci. Comput.* 51 (2012) 650–682.
- [43] K. Mattsson, M. Almquist, A solution to the stability issues with block norm summation by parts operators, *Journal of Computational Physics* 15 (2013) 418–442.
- [44] K. Mattsson, J. Nordström, Summation by parts operators for finite difference approximations of second derivatives, *Journal of Computational Physics* 199 (2004) 503–540.
- [45] K. Mattsson, M. Svard, M. Shoeybi, Stable and accurate schemes for the compressible Navier–Stokes equations, *Journal of Computational Physics* 227 (2008) 2293–2316.
- [46] J. Nordström, J. Gong, E. van der Weide, M. Svård, A Stable and Conservative High Order Multi-block Method for the Compressible Navier-Stokes Equations, *J. Comput. Phys.* 228 (2009) 9020–9035.
- [47] J. Nordström, T. Lundquist, Summation-by-parts in Time, *Journal of Computational Physics* 251 (2013) 487–499.
- [48] M. Osusky, D.W. Zingg, Parallel Newton-Krylov-Schur Solver for the Navier-Stokes Equations Discretized Using Summation-By-Parts Operators, *AIAA Journal* 51 (2013) 2833–2851.
- [49] A. Prothero, A. Robinson, On the stability and accuracy of one-step methods for solving stiff systems of ordinary differential equations, *Mathematics of Computation* 28 (1974) 145–162.
- [50] A. Reichert, M.T. Heath, D.J. Bodony, Energy stable numerical method for hyperbolic partial differential equations using overlapping domain decomposition, *Journal of Computational Physics* 231 (2012) 5243–5265.

- [51] B. Strand, Summation by parts for finite difference approximations for  $d/dx$ , *Journal of Computational Physics* 110 (1994) 47–67.
- [52] M. Svård, On Coordinate Transformations for Summation-by-Parts Operators, *J. Sci. Comput.* 20 (2004) 29–42.
- [53] M. Svård, M.H. Carpenter, J. Nordström, A stable high-order finite difference scheme for the compressible Navier-Stokes equations, far-field boundary conditions, *Journal of Computational Physics* 225 (2007) 1020–1038.
- [54] M. Svård, J. Nordström, A stable high-order finite difference scheme for the compressible Navier-Stokes equations no-slip wall boundary conditions, *Journal of Computational Physics* 227 (2008) 4805–4824.
- [55] M. Svård, J. Nordström, Review of Summation-by-parts schemes for initial-boundary-value problems, *Journal of Computational Physics* 268 (2014) 17–38.